JOURNAL OF THEORETICAL
AND APPLIED MECHANICS
2, 36, 1998

THE BOUNDARY ELEMENT METHOD IN SENSITIVITY ANALYSIS, OPTIMIZATION AND IDENTIFICATION

TADEUSZ BURCZYŃSKI

Department for Strength of Materials and Computational Mechanics, Silesian Technical University
e-mail: burczyns@zesu.polsl.gliwice.pl

This paper deals with applications of the boundary element method to sensitivity analysis, optimization and identification problems. The main motivation is to give a unified exposition with particular reference to the most recent author's numerical results.

Key words: boundary element method, boundary integral equations, sensitivity analysis, shape optimization, defects identification

1. Introduction

The shape determination of structural components plays the essential role in mechanical designing and the problem of shape sensitivity analysis and optimal design is much more complicated than a typical conventional analysis.

For such problems the shape of structural components is treated as a design variable and boundaries are changing during the design process. Finding the best direction of shape change to minimize or maximize a measure of merit of the structure becomes a very important problem in design.

Determination of the effect of shape change of a structural component is the problem of *sensitivity analysis*. The value of shape design sensitivity information is greater than those obtained from conventional analysis with no trend information. To optimize or modify the shape of structural component, the sensitivity analysis for each performance functional is needed and therefore it can be considered as an intermediate step in optimization problems.

In the *shape optimal design* one should determine the shape of the structural component in such a way that an objective functional ought to reach an extremum and constraint have to be satisfied.

A broad class of inverse problems, especially the *identification* problems can also be ranked among the discussed topic because such problems are usually

formulated in such a way that a certain functional must be minimized and therefore these problems can be considered on the basis of sensitivity analysis.

It appears that the Boundary Element Method (BEM) is an exceptionally natural and convenient numerical technique in the shape sensitivity analysis, optimal design and identification.

Current literature on the application of BEM to sensitivity analysis, optimization and identification is expanding explosively. An extensive literature has been developed in this area and its survey is made by Burczyński (1993b).

The main purpose of this paper is to give a concise unified exposition of BEM to the sensitivity analysis, optimization and identification using adjoint variable approach with particular reference to the most recent author's numerical results.

2. Sensitivity analysis

Let a structural component, which is considered as an elastic body, occupy a domain Ω with a boundary Γ. On the boundary Γ are prescribed a field of displacements $\boldsymbol{u}(\boldsymbol{x}) = \boldsymbol{u}^0(\boldsymbol{x})$, $\boldsymbol{x} \in \Gamma_1$ and a field of tractions $\boldsymbol{p}(\boldsymbol{x}) = \boldsymbol{p}^0(\boldsymbol{x})$, $\boldsymbol{x} \in \Gamma_2$ and $\Gamma = \Gamma_1 \cup \Gamma_2$ and $\Gamma_1 \cap \Gamma_2 =$. In the domain Ω there are body forces $\boldsymbol{b}(\boldsymbol{x})$, $\boldsymbol{x} \in \Omega$.

Under specified boundary conditions and applied body forces the body passes from the initial configuration to a deformed one. For small displacement and strain theory, the governing boundary integral equations are described as follows (Burczyński, 1995):

— for displacements

$$\boldsymbol{c}(\boldsymbol{x})\boldsymbol{u}(\boldsymbol{x}) = \int_\Gamma \left[\mathbf{U}^*(\boldsymbol{x},\boldsymbol{y})\boldsymbol{p}(\boldsymbol{y}) - \mathbf{P}^*(\boldsymbol{x},\boldsymbol{y})\boldsymbol{u}(\boldsymbol{y})\right] d\Gamma(\boldsymbol{y}) + \int_\Omega \mathbf{U}^*(\boldsymbol{x},\boldsymbol{y})\boldsymbol{b}(\boldsymbol{y})\, d\Omega(\boldsymbol{y}) \tag{2.1}$$

— for stresses

$$\boldsymbol{\sigma}(\boldsymbol{x}) = \int_\Gamma \left[\mathbf{D}^*(\boldsymbol{x},\boldsymbol{y})\boldsymbol{p}(\boldsymbol{y}) - \mathbf{S}^*(\boldsymbol{x},\boldsymbol{y})\boldsymbol{u}(\boldsymbol{y})\right] d\Gamma(\boldsymbol{y}) + \int_\Omega \mathbf{D}^*(\boldsymbol{x},\boldsymbol{y})\boldsymbol{b}(\boldsymbol{y})\, d\Omega(\boldsymbol{y}) \tag{2.2}$$

where $\mathbf{U}^*$ and $\mathbf{P}^*$ are the fundamental solutions of elastostatics, $\boldsymbol{c}(\boldsymbol{x})$ depends on the local geometry of Γ at $\boldsymbol{x}$, $\mathbf{D}^*$ and $\mathbf{S}^*$ are the third solution tensors obtained after suitable differentiation of $\mathbf{U}^*$ and $\mathbf{P}^*$ with respect to the source point $\boldsymbol{x}$ and application of Hooke's law.

It is obvious that the state fields as displacements $\boldsymbol{u}$, strains $\boldsymbol{\varepsilon}$ and stresses $\boldsymbol{\sigma}$, and an arbitrary performance functional J

$$J = \int_{\Omega} \Psi(\boldsymbol{\sigma}, \boldsymbol{\varepsilon}, \boldsymbol{u})\, d\Omega + \int_{\Gamma} \phi(\boldsymbol{u}, \boldsymbol{p})\, d\Gamma \tag{2.3}$$

where $\Psi(\boldsymbol{\sigma}, \boldsymbol{\varepsilon}, \boldsymbol{u})$ is an arbitrary function of stresses $\boldsymbol{\sigma}$, strains $\boldsymbol{\varepsilon}$ and displacements $\boldsymbol{u}$ within the domain Ω and is an arbitrary function of displacements $\boldsymbol{u}$ and tractions $\boldsymbol{p}$ on the boundary Γ, depend on the shape of Γ.

The performance functional J represents an objective or constraint, and can express different mechanical characteristics and merits of the structure as required as well as local stress, strains, displacements and tractions at an arbitrary point $\boldsymbol{x}_0$, for example in some shape optimization or identification context.

The objective of sensitivity analysis is to determine the dependency of the state fields $\boldsymbol{q}$ ($\boldsymbol{q} = \boldsymbol{u}, \boldsymbol{\varepsilon}, \boldsymbol{\sigma}$) and, in the general case, the functional J on the shape of Γ.

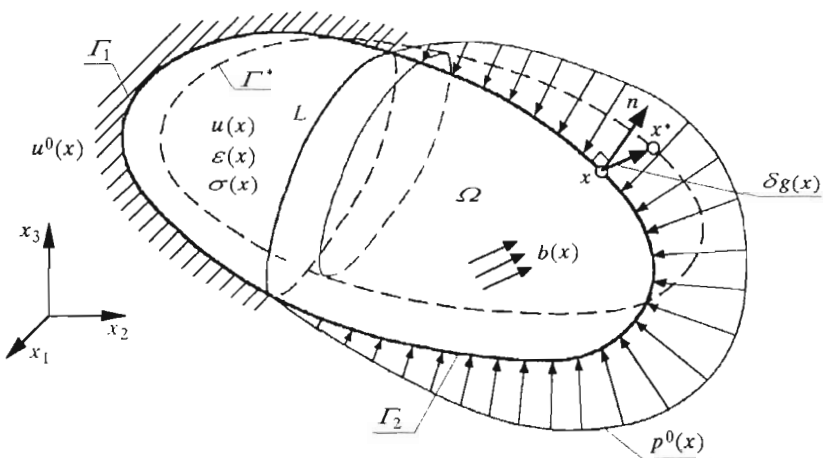

Fig. 1. Primary system and shape transformation of its boundary

Consider an infinitesimal variation of configuration of the body by prescribing a continuous and differentiable vector field $\delta \boldsymbol{g}(\boldsymbol{x})$, so that (Fig.1)

$$\boldsymbol{x}^* = \boldsymbol{x} + \delta \boldsymbol{g}(\boldsymbol{x}) \tag{2.4}$$

The transformation field $\boldsymbol{g}(\boldsymbol{x}) = \boldsymbol{g}(\boldsymbol{x}, \boldsymbol{a})$ modifies the shape of the boundary Γ, where $\boldsymbol{a} = (a_r)$, $r = 1, 2, ..., R$, is the set of shape design parameters which

specify the actual shape of the structure. The co-ordinates of boundary nodes, control points of Bezier functions or B-splines or some dimensions of the body can be chosen as the shape parameters. The variable $\boldsymbol{x}$ is defined in the untransformed domain Ω with the boundary Γ and variable $\boldsymbol{x}^*$ is defined in the transformed domain $\Omega^* = \Omega(\boldsymbol{a})$ with the boundary $\Gamma^* = \Gamma(\boldsymbol{a})$.

The first variation of the transformation field $\boldsymbol{g}(\boldsymbol{x})$ is expressed as

$$\delta \boldsymbol{g} = \boldsymbol{v}^r \delta a_r \tag{2.5}$$

where $\boldsymbol{v}^r = \partial \boldsymbol{g}/\partial \boldsymbol{a}_r$ can be considered as a transformation velocity field which is associated with a shape design parameter a_r.

The first derivative with respect to the shape parameters $\boldsymbol{a} = (a_r)$ can be expressed analytically (see Mróz, 1986)

$$\begin{aligned}\frac{DJ}{Da_r} &= \int_\Gamma \Big[\Psi - \boldsymbol{\sigma}\boldsymbol{\varepsilon}^a + \boldsymbol{b}\boldsymbol{u}^a + (\phi + \boldsymbol{p}\boldsymbol{u}^a)_{,n} K\Big] n_k v_k^r \, d\Gamma + \\ &+ \int_{\Gamma_1} \Big(\frac{\partial \phi}{\partial \boldsymbol{u}} - \boldsymbol{p}^a\Big)\Big(\frac{D\boldsymbol{u}^0}{Da_r} - \boldsymbol{u}^0_{,k} v_k^r\Big) \, d\Gamma_1 + \\ &+ \int_{\Gamma_2} \Big(\frac{\partial \phi}{\partial \boldsymbol{p}} + \boldsymbol{u}^a\Big)\Big(\frac{D\boldsymbol{p}^0}{Da_r} - \boldsymbol{p}^0_{,k} v_k^r\Big) \, d\Gamma_2 + \int_L \|\phi + \boldsymbol{p}\boldsymbol{u}^a\| v_\nu^r \, dL\end{aligned} \tag{2.6}$$

where $\|\phi + \boldsymbol{p}\boldsymbol{u}^a\| = (\phi + \boldsymbol{p}\boldsymbol{u}^a)^+ - (\phi + \boldsymbol{p}\boldsymbol{u}^a)^-$ represents the discontinuity of $(\phi + \boldsymbol{p}\boldsymbol{u}^a)$ along the curve L, which separates two parts of the boundary Γ_1 and Γ_2, $\boldsymbol{n} = [n_k]$ is the unit normal vector, K is the mean curvature of the boundary.

The analytical expression for sensitivity of the functional J depends on the primary solution (PS): $\boldsymbol{u}$, $\boldsymbol{\varepsilon}$, $\boldsymbol{\sigma}$ and the adjoint solution (AS): $\boldsymbol{u}^a$, $\boldsymbol{\varepsilon}^a$ and $\boldsymbol{\sigma}^a$. The adjoint system is an elastic body with the same configuration and physical properties as the primary system but with the other boundary conditions

$$\boldsymbol{u}^{a0} = -\frac{\partial \phi(\boldsymbol{u}, \boldsymbol{p})}{\partial \boldsymbol{p}} \quad \text{on } \Gamma_1 \qquad \boldsymbol{p}^{a0} = \frac{\partial \phi(\boldsymbol{u}, \boldsymbol{p})}{\partial \boldsymbol{u}} \quad \text{on } \Gamma_2 \tag{2.7}$$

and with the initial strains $\boldsymbol{\varepsilon}^{ai}$, stresses $\boldsymbol{\sigma}^{ai}$ fields and body forces $\boldsymbol{b}$ specified within the domain Ω

$$\boldsymbol{\varepsilon}^{ai} = \frac{\partial \Psi(\boldsymbol{\sigma}, \boldsymbol{\varepsilon}, \boldsymbol{u})}{\partial \boldsymbol{\sigma}} \qquad \boldsymbol{\sigma}^{ai} = \frac{\partial \Psi(\boldsymbol{\sigma}, \boldsymbol{\varepsilon}, \boldsymbol{u})}{\partial \boldsymbol{\varepsilon}} \qquad \boldsymbol{b}^{ai} = \frac{\partial \Psi(\boldsymbol{\sigma}, \boldsymbol{\varepsilon}, \boldsymbol{u})}{\partial \boldsymbol{u}} \tag{2.8}$$

The boundary integral equations for the primary and adjoint systems, respectively, have the form

$$\boldsymbol{c}(x)u^w(x) = \int_\Gamma \left[\mathsf{U}^*(x,y)p^w(y) - \mathsf{P}^*(x,y)u^w(y)\right] d\Gamma(y) + \mathsf{B}^w(x) \tag{2.9}$$

$$w = (PS),(AS)$$

where $\mathbf{B}^w$ depends on the body forces in the case of the primary system and on the initial strains ε^{ai}, stresses $\boldsymbol{\sigma}^{ai}$ and body forces $\boldsymbol{b}^{ai}$ in the case of the adjoint system.

It is worth noting that the analytical expression for sensitivity of the functional J depends on only one additional adjoint boundary solution independent of the number of shape design parameters. The fact that the final expression for sensitivity of the arbitrary function J depends only on boundary state variables of the primary and adjoint systems brings significant advantages in numerical calculations by means of BEM. It is well known that BEM is the most suitable for applications involving high accuracy of the boundary stresses. Therefore, boundary elements are most naturally suited to design sensitivity implementations.

The presented approach to shape sensitivity analysis using BEM has been implemented numerically and its accuracy and efficiency have been examined (cf Burczyński et al., 1995, 1997b).

If the body contains a defect (a void or a crack) especially with a singular boundary Γ_0, and we are interested in the sensitivity of J with respect to shape transformation of Γ_0, then it is convenient to consider a special kind of shape transformation in the form:

- *translation* (T), by prescribing variations δb_k, $k = 1,2,3$, where b_k are translation parameters,
- *rotation* (R), by prescribing $\delta\omega_p$, $p = 1,2,3$, where ω_p are rotation parameters,
- *scale change (expansion or contraction)* (S), by prescribing $\delta\eta$, where η is a scale change parameter.

The first variation of J is expressed by path independent integrals along an arbitrary closed surface (for 3D) or contour (for 2D problems) Γ_* enclosing the defect (Dems and Mróz, 1986)

$$\frac{DJ}{Da_q} = \int_{\Gamma_*} Z_L^q(\sigma,\varepsilon,\boldsymbol{u},\boldsymbol{\sigma}^a,\varepsilon^a,\boldsymbol{u}^a)\, d\Gamma_* \qquad L = T,R,S \quad q = 1,2,...,Q \tag{2.10}$$

where $\boldsymbol{\sigma}$, $\boldsymbol{\varepsilon}$, $\boldsymbol{u}$ are stress, strain and displacement fields for the primary problem, respectively, and $\boldsymbol{\sigma}^a$, $\boldsymbol{\varepsilon}^a$, $\boldsymbol{u}^a$ are the same fields for the adjoint problem.

Integrands Z_L^q depend on the state fields of primary and adjoint solutions:
— for translation $(k = 1, 2, 3)$

$$Z_T^k = (\Psi \delta_{kj} + \sigma_{ij} u^a_{i,k} + \sigma^a_{ij} u_{i,k} - \sigma_{il} \varepsilon^a_{il} \delta_{kj}) n_j \tag{2.11}$$

— for rotation $(p = 1, 2, 3)$

$$Z_R^{p+3} = e_{kpl}(\Psi x_l \delta_{kj} - \sigma_{iq} \varepsilon^a_{iq} x_l \delta_{kj} + \sigma_{ij} u^a_{i,k} x_l + \sigma_{lj} u^a_k + \sigma^a_{lj} u_k + \sigma^a_{ij} u_{i,k} x_l) n_j \tag{2.12}$$

— for expansion or contraction

$$Z_S^7 = \Big[\frac{2}{\alpha} \sigma^a_{ij} u_i + \Big(\frac{2}{\alpha} - \beta\Big) \sigma_{ij} u^a_i + x_k \sigma^a_{ij} u_{i,k} - x_k \sigma_{ij} u^a_{i,j} \delta_{jk} + x_k \sigma_{ij} u^a_{i,k}\Big] n_j \tag{2.13}$$

Eq (2.13) was derived for $\Psi = 0$ and for a homogeneous function $\phi(\boldsymbol{u}, \boldsymbol{p}) = \phi(\boldsymbol{u})$ of the order $\alpha, \beta = 1$ for 3D and $\beta = 0$ for 2D, n_j is a component of the unit normal vector to the contour Γ_*.

It is seen from Eqs (2.10)÷(2.13) that in order to calculate derivatives of an arbitrary functional J with respect to translations, rotations and expansion it is enough to calculate the path-independent integrals along an arbitrary surface Γ_* enclosing the crack or the void. In the particular case the surface Γ_* can be identified with the external boundary Γ and the sensitivity information is obtained using only the boundary integral equations.

In the case of several voids or cracks the path-independent integrals can also be applied to sensitivity analysis with respect to translation, rotation and scale change of each particular defect. In this case when each void or crack is surrounded independently by a closed surface Γ_*^i not penetrating the other voids and the path-independent integrals associated with the respective shape transformation is calculated along this surface.

In the case when the body contains a crack in the form a traction-free linear cut with zero thickness it is possible to use for 2D problems special fundamental solutions which include the exact solution for such a crack. For this approach the crack is not discretized by boundary elements but only the external boundary.

For any arbitrary crack if we use the *dual boundary element method* it is necessary to apply an additional hypersingular vector boundary integral equation for tractions (Portela, 1993)

$$\frac{1}{2} \boldsymbol{p}^w(\boldsymbol{x}) = \boldsymbol{n}(\boldsymbol{x}) \int_\Gamma \mathbf{D}^*(\boldsymbol{x}, \boldsymbol{y}) \boldsymbol{p}^w(\boldsymbol{x})\, d\Gamma(\boldsymbol{y}) - \boldsymbol{n}(\boldsymbol{x}) \int_\Gamma \mathbf{S}^*(\boldsymbol{x}, \boldsymbol{y}) \boldsymbol{u}^w(\boldsymbol{y})\, d\Gamma(\boldsymbol{y}) \tag{2.14}$$

Eq (2.14) is applied to source points on the one part of the crack boundary.

One can expect that calculations of sensitivity of J by means of path-independent integrals along a fixed surface (contours for 2D), far from singularities caused by the crack or void, ensure a good accuracy of these derivatives. This feature is very useful in the shape optimal design of voids, topology optimization and defect identification. The path-independent and boundary integrals for sensitivity of boundary displacements have been tested numerically for several 2D problems of elasticity with internal cracks and voids (cf Burczyński et al., 1996a,b, 1997a; Burczyński and Polch, 1994).

The discrete versions of the boundary integral equations (2.9) are obtained from approximation the boundary by series of boundary elements Γ^e, $e = 1, 2, ..., E$. The boundary displacements and tractions are approximated over each boundary element Γ^e by means of nodal values and interpolation functions. Finally, the discrete version of boundary integral equations takes the form

$$\mathbf{H}\mathbf{U}^w = \mathbf{G}\mathbf{P}^w + \mathbf{Z}^w \qquad w = (PS), (AS) \tag{2.15}$$

where $\mathbf{U}^w$ and $\mathbf{P}^w$ are column matrices of nodal displacements and tractions, respectively, $\mathbf{H}$ and $\mathbf{G}$ are square matrices which depend on boundary integral of fundamental solutions, interpolations functions and jacobians. $\mathbf{Z}^w$ is a column matrix dependent on the body forces $\boldsymbol{b}$, in the case of the primary system, or on body forces $\boldsymbol{b}^a$, initial strains $\boldsymbol{\varepsilon}^{ai}$ and stresses $\boldsymbol{\sigma}^{ai}$, in the case of the adjoint system. It is worth noting that $\mathbf{H}$ and $\mathbf{G}$ are the same for the primary system as well as the adjoint system, and therefore are calculated only once. Taking into account the boundary conditions Eq (2.15) can be reordered in such a way that all unknown variables are written in the column matrix $\mathbf{X}^w$ and known variables in $\mathbf{Y}^w$. The final form can be written

$$\mathbf{A}\mathbf{X}^w = \mathbf{B}\mathbf{Y}^w + \mathbf{Z}^w \qquad w = (PS), (AS) \tag{2.16}$$

Solving Eq (2.16) one obtains the state fields of the primary and adjoint systems, which are required to calculate sensitivities of the functional J.

The application of BEM to shape sensitivity analysis of dynamic transient problems was considered by Burczyński and Fedeliński (1992). In this section only the sensitivity analysis for free vibration of elastic bodies is present. The sensitivity of natural frequency w can be expressed by Burczyński and Fedeliński (1990a)

$$\frac{D\omega}{Da_r} = \int_{\Gamma} \left[\boldsymbol{\sigma}(\boldsymbol{u})\boldsymbol{\varepsilon}(\boldsymbol{u}) - \omega^2 \rho \boldsymbol{u}\boldsymbol{u} \right] n_k v_k^r \, d\Gamma \tag{2.17}$$

It is interesting to notice that the sensitivity of natural frequency with respect to the shape of the body is given by the boundary integral and depends on the natural frequency and modes $\boldsymbol{u}(\boldsymbol{x})$ determined on the boundary.

The eigenvalue problem is solved using the dual reciprocity BEM approach. The displacement amplitude $\boldsymbol{u}(\boldsymbol{x})$ within the domain is approximated by using a set of unknown coefficients $\boldsymbol{s}^m$ and a set of coordinate functions $f(\boldsymbol{x})$

$$\boldsymbol{u}(\boldsymbol{x}) = \boldsymbol{s}^m f^m(\boldsymbol{x}) \qquad m = 1, 2, ..., M \tag{2.18}$$

The equation of free vibrations may be written in the boundary integral form

$$\boldsymbol{c}(\boldsymbol{x})\boldsymbol{u}(\boldsymbol{x}) - \int_\Gamma \left[\mathbf{U}^*(\boldsymbol{x},\boldsymbol{y})\boldsymbol{p}(\boldsymbol{y}) - \mathbf{P}^*(\boldsymbol{x},\boldsymbol{y})\boldsymbol{u}(\boldsymbol{y})\right] d\Gamma(\boldsymbol{y}) +$$

$$+\omega^2\rho\left\{\boldsymbol{c}(\boldsymbol{x})\widehat{\boldsymbol{u}}^m(\boldsymbol{x}) - \int_\Gamma \left[\mathbf{U}^*(\boldsymbol{x},\boldsymbol{y})\widehat{\boldsymbol{p}}^m(\boldsymbol{y}) - \mathbf{P}^*(\boldsymbol{x},\boldsymbol{y})\widehat{\boldsymbol{u}}^m(\boldsymbol{y})\right] d\Gamma(\boldsymbol{y})\boldsymbol{s}^m\right\} = 0 \tag{2.19}$$

where $\mathbf{U}^*$ and $\mathbf{P}^*$ are fundamental solutions of elastostatics, $\widehat{\boldsymbol{u}}^m$ and $\widehat{\boldsymbol{p}}^m$ and are pseudo-fields of displacements and tractions, respectively, resulting from the pseudo-body force $\mathbf{I}f^m$ ($\mathbf{I}$ - unit matrix).

After discretization Eq (2.19) takes the algebraic form

$$\mathbf{HU} = \omega^2\mathbf{MU} \tag{2.20}$$

where the mass matrix $\mathbf{M}$ is given by

$$\mathbf{M} = -\rho[\mathbf{H}\widehat{\mathbf{U}} - \mathbf{G}\widehat{\mathbf{P}}]\mathbf{F} \tag{2.21}$$

$\mathbf{H}$ and $\mathbf{G}$ are the same matrices as for static problems, while $\widehat{\mathbf{U}}$ and $\widehat{\mathbf{P}}$ contain the nodal values of functions $\widehat{\boldsymbol{u}}$ and $\widehat{\boldsymbol{p}}$, respectively, and the matrix $\mathbf{F}$ depends on the nodal values of functions $f^m(\boldsymbol{x})$.

Several numerical tests have been performed using Eq (2.17) and dual BEM (see Burczyński and Fedeliński, 1990b; Fedeliński, 1991).

3. Shape optimization

The problem of shape optimal design consists in finding the optimum shape design parameters $\boldsymbol{a}_{op}$ according to a prescribed optimality criterion. The functional J, Eq (2.3), can express various objective or constraint functionals (cf Burczyński, 1993a; Burczyński et al., 1995).

A well-posed optimal shape design problem stated as:

- minimize an objective functional $J_0(\boldsymbol{a})$ with the behaviour constraints J_α, $\alpha = 1, 2, ..., A$, imposed expressed in terms of stresses, strains, displacements and with the upper bound of the cost of the structure J_c, that is

$$J_0(\boldsymbol{a}) \to \min_{\boldsymbol{a}} \tag{3.1}$$

subject to the constraint

$$J_\alpha - c_\alpha \leq 0 \qquad \alpha = 1, 2, ..., A \tag{3.2}$$

where c_α are given constants.

If the cost of the structure is treated as proportional to the material volume or weight, one can write

$$J_c = \int_\Omega C \, d\Omega \tag{3.3}$$

where C is the specific cost of a material.

An alternative formulation of the shape design problem requires minimization of the cost structure $J_0 = J_c$ with the behaviour constraints imposed.

In order to solve the formulated shape optimization problem two approaches can be employed:

– optimality condition methods,

– mathematical programming methods.

Application of the optimality condition methods involves two distinct steps. The first step consists in derivation of the necessary optimality conditions. The problem is replaced by the problem of finding the stationarity point of the Lagrangean functional L

$$L = J_0 + \sum_{\alpha=1}^{A} \lambda_\alpha (J_\alpha - c_\alpha) \tag{3.4}$$

where λ_α $(\alpha = 1, 2, ..., A)$ are the Langrange multipliers $(\lambda_\alpha \geq 0)$.

Now the stationarity condition of L is expressed as follows

$$\delta L = \delta J_0 + \sum_{\alpha=1}^{A} \lambda_\alpha \delta J_\alpha = 0 \qquad \lambda_\alpha (J_\alpha - c_\alpha) = 0 \tag{3.5}$$

In the second step an efficient iterative procedure is constructed to achieve these conditions. Using this approach the problem is reduced to evaluating the state fields of the primary and adjoint systems and unknown optimal shape parameters $\boldsymbol{a}_{op} = (a_r)$, $r = 1, 2, ..., R$, and the Lagrange multipliers λ_α $(\alpha = 1.2, ..., A)$.

In the typical mathematical programming application the search for the optimum shape parameters $\boldsymbol{a}_{op}$ is based on the construction of iterative process of the type

$$\boldsymbol{a}^{(i+1)} = \boldsymbol{a}^{(i)} + \beta^{(i)} \boldsymbol{h}^{(i)} \tag{3.6}$$

where $\boldsymbol{h}^{(i)}$ is the vector determining the direction of motion from the point $\boldsymbol{a}^{(i)}$ to $\boldsymbol{a}^{(i+1)}$ and $\beta^{(i)}$ is a numerical factor whose value determines the length of the step in the direction of $\boldsymbol{h}^{(i)}$.

There are several numerical optimization techniques which enable one to construct the iterative process (3.6). There are effective methods in which the vector $\boldsymbol{h}^{(i)}$ depends only on gradients of the objective and constraint functionals. In this case the sensitivity information can be directly applied.

In most shape optimization problem of vibrating structures one should maximize the fundamental circular frequency with geometrical and cost constraints. Thus, the problem is to find shape parameters a_r, $r = 1, 2, ..., R$, that minimize

$$J_0 = -\omega \to \min_{\boldsymbol{a}} \tag{3.7}$$

subject to the cost constraints.

The aim of the optimization can be also maximization of the minimum difference between forcing frequency ω_f and natural frequencies ω_i (Fedeliński, 1991)

$$J_0 = \max_{\boldsymbol{a}} \Big(\min |\omega_f - \omega_i| \Big) \tag{3.8}$$

Recently, new capabilities of BEM in topology optimization have been proposed, Burczyński et al. (1996a), Burczyński and Kokot (1997).

BEM formulation offers the distinct advantages:

(i) in the iteratively optimal design process one uses only the values defined on the modified boundary,

(ii) if it is necessary the boundary element mesh can easily be generated and design changes do not require a complete remeshing.

4. Identification

The boundary and path-independent integrals mentioned above can be applied to identification problems where the location and size of a defect (a crack or a void) are to be determined through the measurements of boundary displacements. One assumes that a given body contains an interior defect with the boundary Γ_0 whose shape and location are unknown.

One should determine the geometry of the defect basing on available measurement data of displacements $\widehat{\boldsymbol{u}}^m$ at boundary points $\boldsymbol{x}^m$, $m = 1, 2, ..., M$. In order to solve this problem a boundary displacement functional is constructed. This functional represents a distance norm between the measured $\widehat{\boldsymbol{u}}^m$ and theoretical values of displacements $\boldsymbol{u}(\boldsymbol{x}_m)$ calculated at discrete boundary points $\boldsymbol{x}_m$

$$J = \frac{1}{2} \sum_{m=1}^{M} \left[\boldsymbol{u}(\boldsymbol{x}_m) - \widehat{\boldsymbol{u}}^m \right]^2 = \int_{\Gamma} \varphi(\boldsymbol{u}) \, d\Gamma \tag{4.1}$$

where

$$\varphi(\boldsymbol{u}) = \frac{1}{2} \sum_{m=1}^{M} \left[\boldsymbol{u}(\boldsymbol{x}_m) - \widehat{\boldsymbol{u}}^m \right]^2 \delta(\boldsymbol{x} - \boldsymbol{x}^m) \tag{4.2}$$

The size and position of the defect are described by a set of shape parameters $\boldsymbol{a} = (a_q)$, $q = 1, 2, ..., Q$, which describe translation, rotation and scale change, respectively, of a given initial defect.

In order to solve this problem one should find the vector $\boldsymbol{a}$ which minimizes the objective function $J = J(\boldsymbol{a})$ given by Eq (4.1).

To have a physical meaning, the defect specified by vector $\boldsymbol{a}$ must lie completely inside the body. This condition is satisfied in the minimization process through imposing geometric constraints which can be expressed symbolically in the form

$$C_j(a_q) \leq 0 \qquad j = 1, 2, ..., L \qquad q = 1, 2, ..., Q \tag{4.3}$$

The constraints (4.3) together with minimization of the objective function J, Eq (4.1), lead to the nonlinear constrained optimization problem. For transforming this problem into an unconstrained optimization problem, one can propose the internal penalty function method. The augmented objective function for this case has the form

$$\widehat{J}(\boldsymbol{a}, r) = J(\boldsymbol{a}) + P[C_j(a_q), r] \tag{4.4}$$

where P denotes the internal penalty function and depends upon the constraints C_j as well as upon an arbitrary penalty parameter r.

The internal penalty function approaches minimum from the points lying inside the feasible region and depicts a good performance. This function can be expressed as follows

$$P[C_j(a_q), r] = r \sum_{j=1}^{L} \sum_{q=1}^{Q} \frac{1}{C_j(a_q)} \tag{4.5}$$

The identification of the defect as an inverse problem is ill-posed and its solution may not be stable since small errors in the experimentally measured displacements may result in a significant difference in the computed defect geometry. Regularization methods can reduce the numerical fluctuations in the solution by modifying the objective function. The augmented regularization terms, up to the second order terms, can be expressed in the form

$$R = \frac{\gamma_0}{2} \sum_{q=1}^{Q} \left[a_q^{(n)}\right]^2 + \frac{\gamma_1}{2} \sum_{q=1}^{Q} \left[a_q^{(n)} - a_q^{(n-1)}\right]^2 + \frac{\gamma_2}{2} \sum_{q=1}^{Q} \left[a_q^{(n)} - 2a_q^{(n-1)} + a_q^{(n-2)}\right]^2 \tag{4.6}$$

where γ_j are the regularization parameters, and n is the iteration number.

Now, the final augmented objective function can be expressed in the form

$$\widehat{J}(\boldsymbol{a}, r) = J(\boldsymbol{a}) + P[C_j(a_q), r] + R \tag{4.7}$$

The size and position of the defect are calculated iteratively using Eq (3.6).

In order to solve the identification problem one should establish the method of choosing the vector $\boldsymbol{h}^{(i)}$ which depends on gradient of the augmented objective function $\widehat{J}$.

Taking into account Eqs (4.1), (4.2), (4.5), and (4.6), the gradient of the final augmented objective function is expressed by the sensitivity of $\widehat{J}$ with respect to the shape design parameters

$$\begin{aligned} \frac{D\widehat{J}}{D\boldsymbol{a}} = \frac{DJ}{D\boldsymbol{a}} + r \sum_{j=1}^{L} \Big[& -\frac{1}{C_{jx}^2(x)} \frac{\partial C_{jx}(x)}{\partial x} \frac{\partial x}{\partial \boldsymbol{a}} + \\ & -\frac{1}{C_{jy}^2(y)} \frac{\partial C_{jy}(x)}{\partial y} \frac{\partial y}{\partial \boldsymbol{a}} - \frac{1}{C_{jz}^2(z)} \frac{\partial C_{jz}(z)}{\partial z} \frac{\partial z}{\partial \boldsymbol{a}} \Big] + \\ & +\gamma_0 \sum_{q=1}^{Q} a_q^{(n)} + \gamma_1 \sum_{q=1}^{Q} \left[a_q^{(n)} - a_q^{(n-1)}\right] + \gamma_2 \sum_{q=1}^{Q} \left[a_q^{(n)} - 2a_q^{(n-1)} + a_q^{(n-2)}\right] \end{aligned} \tag{4.8}$$

where $\partial x/\partial \boldsymbol{a}$, $\partial y/\partial \boldsymbol{a}$ and $\partial z/\partial \boldsymbol{a}$ are sensitivities of the x, y and z coordinates of the defect geometry (3D case), respectively. Derivatives $DJ/D\boldsymbol{a}$ are calculated from Eq (2.10) when $\Psi = 0$ in Eqs (2.11) and (2.12).

The boundary conditions for the adjoint system are given as follows

$$\boldsymbol{u}^{a0} = -\frac{\partial \varphi(\boldsymbol{u})}{\partial \boldsymbol{p}} \qquad \text{on } \Gamma_1 \qquad (4.9)$$

$$\boldsymbol{p}^{a0} = \frac{\partial \varphi(\boldsymbol{u})}{\partial \boldsymbol{u}} \sum_{m=1}^{M} \left[\boldsymbol{u}(\boldsymbol{x}_m) - \widehat{\boldsymbol{u}}^m\right] \delta(\boldsymbol{x} - \boldsymbol{x}^m) \qquad \text{on } \Gamma_2 \qquad (4.10)$$

It means that the adjoint system should be loaded by a system of concentrated forces $\sum_{m=1}^{M}[\boldsymbol{u}(\boldsymbol{x}_m) - \widehat{\boldsymbol{u}}^m]\delta(\boldsymbol{x} - \boldsymbol{x}^m)$ acting at the boundary points $\boldsymbol{x}^m$.

The presented above method of identification has been used to identification of voids and cracks in static elastic structures (cf Burczyński et al., 1996a, 1996b; Burczyński and Polch, 1994). It is possible to extend this approach also onto identification in vibration problems (see Burczyński et al., 1997c; Burczyński and Nowakowski, 1997).

5. Numerical examples

To demonstrate the accuracy and efficiency of BEM, a series of sample solutions is presented.

Example 1. *Sensitivity analysis for 3D elastic body (see Burczyński et al., 1995)*

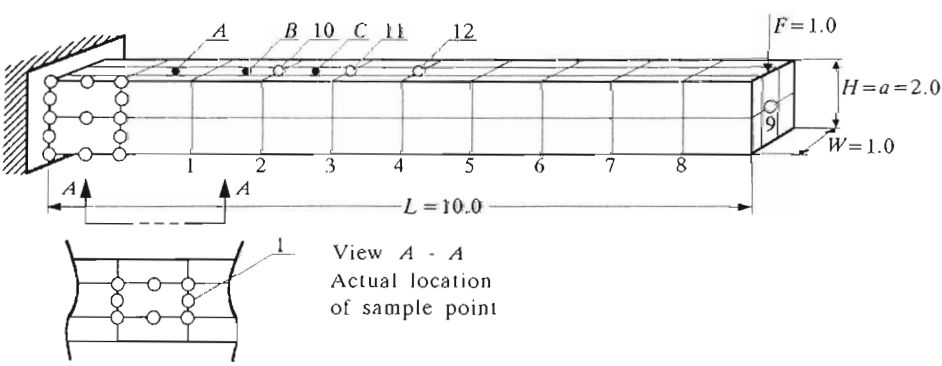

Fig. 2. 3D elastic body

Sensitivity analysis for a transversly loaded cantilever 3D beam with a rectangular cross section was performed. The geometry, boundary element model, loading, and response sensitivity sample point locations associated with this problem are depicted in Fig.2. As a design variable the height a was chosen in this case. The boundary element model had 112 quadrilateral surface elements and 338 nodes.

Table 1 contains the computed results of sensitivity analysis of the global (complementary energy, displacement functional) and sensitivities of vertical (u_2), horizontal (u_1) displacements and a membrane components of the local stress tensor at selected sample points. Note that the displacements functional defined by Eq (5.3) used $u_0 = 936.1$ and $k = 2$.

Table 1. Numerical results of sensitivities of global and local functionals for a 3D elastic body

Point	Functional/state field	Sensitivity analysis	Finite difference	$\delta\%$
	complementary energy	−1876.08	−1917.50	2.16
	displacement functional	−6.40	−6.76	5.39
1	$\boldsymbol{u}_{2,a}$	34.52	34.00	1.53
2	$\boldsymbol{u}_{2,a}$	76.23	78.00	3.51
3	$\boldsymbol{u}_{2,a}$	132.73	140.00	5.19
4	$\boldsymbol{u}_{2,a}$	201.92	210.00	3.85
5	$\boldsymbol{u}_{2,a}$	281.56	290.00	2.91
6	$\boldsymbol{u}_{2,a}$	369.41	385.00	4.05
7	$\boldsymbol{u}_{2,a}$	463.31	480.00	3.48
8	$\boldsymbol{u}_{2,a}$	560.79	585.00	4.13
9	$\boldsymbol{u}_{2,a}$	656.10	673.81	2.63
9	$\boldsymbol{u}_{1,a}$	33.24	33.67	1.28
10	$\boldsymbol{u}_{1,a}$	−32.60	−35.00	6.86
11	$\boldsymbol{u}_{1,a}$	−41.70	−44.00	5.23
12	$\boldsymbol{u}_{1,a}$	−49.30	−51.50	4.27
A	$\overline{\sigma}_{11,a}$	−12.15	−12.37	1.82
B	$\overline{\sigma}_{11,a}$	−11.04	−10.81	2.13
C	$\overline{\sigma}_{11,a}$	−9.71	−9.26	3.78

In Table 1, the results are compared with sensitivities obtained by the finite difference procedure. Note good agreement of the sensitivity analysis and finite difference approaches for this problem. The relative error $\delta\%$ is given by comparing sensitivity analysis and finite difference.

Example 2. *Sensitivity analysis for voids (see Burczyński et al., 1996b)*

The sensitivity analysis was carried out for a rectangular plate with different shapes of internal void. Functional was defined as vertical displacements u_2 at the boundary point $\boldsymbol{x}_0$ where the load $\boldsymbol{p}$ was applied (Fig.3).In order to obtain satisfactory numerical results of displacements sensitivities, a special adaptive integration procedure was used in calculation of path-independent integrals. Derivatives of vertical displacements with respect to translations, rotation and expansion of the voids were calculated for many different internal voids; namely, a circle, an ellipse, a triangle and a square (Table 2).These derivatives were calculated for the same trapezoidal contour. Derivatives of the vertical displacement with respect to translations, rotation and expansion of the triangle void were also calculated for many different contours to verify numerical path-independence of these integrals. Numerical calculations showed a very good agreement for all types of contours.

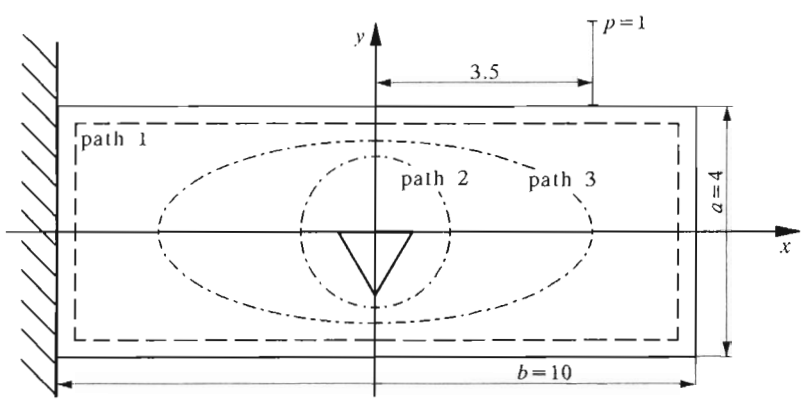

Fig. 3. Different contours for a triangle void

Table 2. Numerical results of sensitivities for different defects using trapezoidal contour (P-II – path-independent integrals; FDI – finite difference information)

Void shape	Method	$\frac{Du_2}{Db_1} \times 10^2$	$\frac{Du_2}{Db_2} \times 10^2$	$\frac{Du_2}{D\omega_3} \times 10^2$	$\frac{Du_2}{D\eta}$
circle	P-II	−0.1723	−0.1613	$-0.5395 \cdot 10^{-5}$	0.1040
$r = 1$; center=(0,0)	FD	−0.1759	0.1583	$0.2526 \cdot 10^{-4}$	0.1040
ellipse	P-II	−0.1025	$-0.5452 \cdot 10^{-1}$	$0.1516 \cdot 10^{-1}$	$0.2289 \cdot 10^{-1}$
x-width=0.2	FD	−0.1154	$-0.5291 \cdot 10^{-1}$	$0.1436 \cdot 10^{-1}$	$0.2307 \cdot 10^{-1}$
y-width=1					
triangle	P-II	$-0.5719 \cdot 10^{-1}$	−0.3618	0.1374	$0.1247 \cdot 10^{-1}$
corners= (−0.5, 0);	FD	$-0.6153 \cdot 10^{-1}$	−0.3753	0.1362	$0.1258 \ 10^{-1}$
(0.5, 0); (0, −1)					
square	P-II	−0.2583	−0.2889	−0.1710	0.3050
center=(0,0)	FD	−0.2725	−0.2832	−0.1679	0.3043
corner=(1,1)					

Example 3. *Sensitivity analysis of natural frequencies (see Burczyński and Fedeliński, 1990b)*

A steel rectangular rigid supported plate was examined to demonstrate the sensitivity analysis of natural frequencies. The plate was divided into 50 linear boundary elements (Fig.4a). The sensitivities of natural frequencies caused by modification of the lower boundary were calculated. In order to check the sensitivity accuracy, the variations of three lowest circular frequencies dw caused by the normal interior modification equal to $\delta a = 0.1$ m were compared with the finite differences $\Delta\omega$. The variations were divided by the variations of the plate area $\delta\Omega$. Due to symmetry the results for one-half of the plate are shown in Fig.4b. It can be seen that the comparison of the predicted variations and differences yields good agreement. The modification of the boundary in the neighbourhood of the support reduces natural frequencies.

Example 4. *Shape optimization of a steel corner for minimum compliance (see Burczyński, 1993a)*

The problem of shape optimal design for minimum compliance which is expressed by the complementary energy

$$J_0 = \frac{1}{2} \int_{\Omega} \boldsymbol{\sigma\varepsilon} \, d\Omega - \int_{\Gamma_1} \boldsymbol{pu}^0 \, d\Gamma_1 \tag{5.1}$$

with the upper bound on the are for a steel corner was considered. The boundary element model consist of 28 linear elements (Fig.5a). The iterative

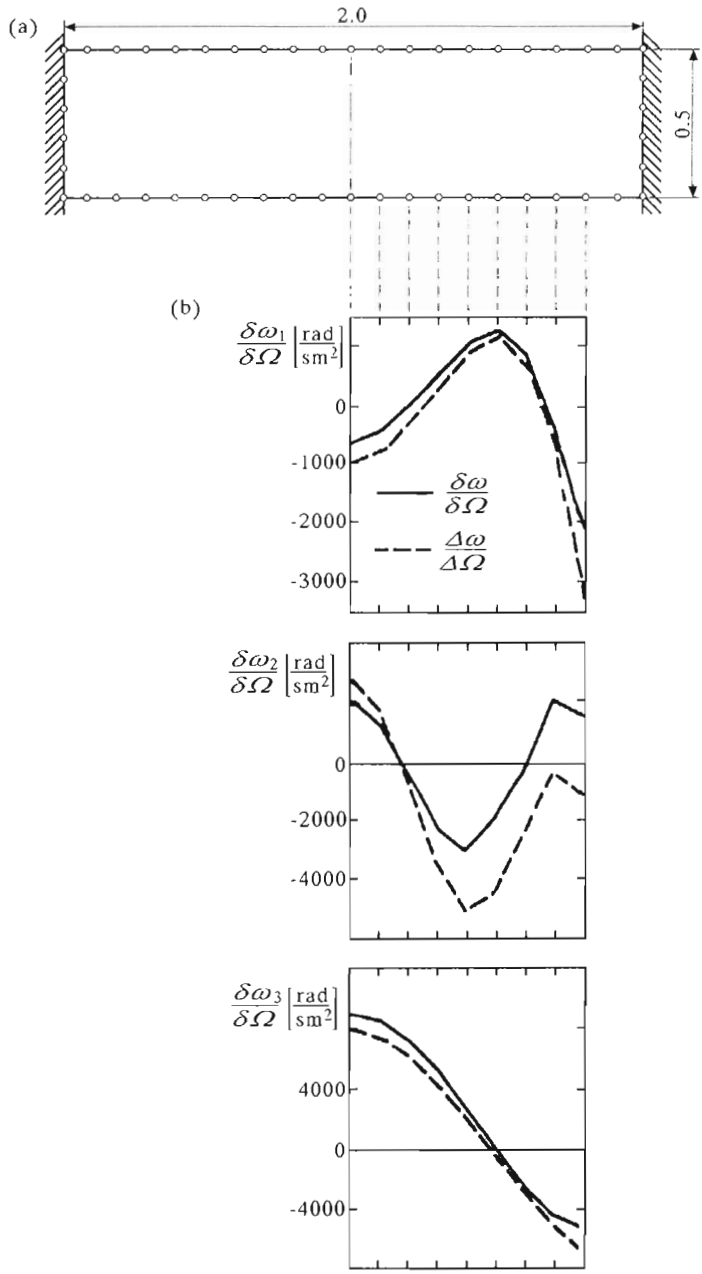

Fig. 4. Sensitivity analysis of natural frequencies

optimization process ended in 12 iterations. The area of the body was practically constant. The distribution of the Von Mises equivalent stresses on the optimization boundary before and after optimization, respectively, are is presented in Fig.5b. It is worth noting that the equivalent stresses are equalized on the optimal boundary of the corner.

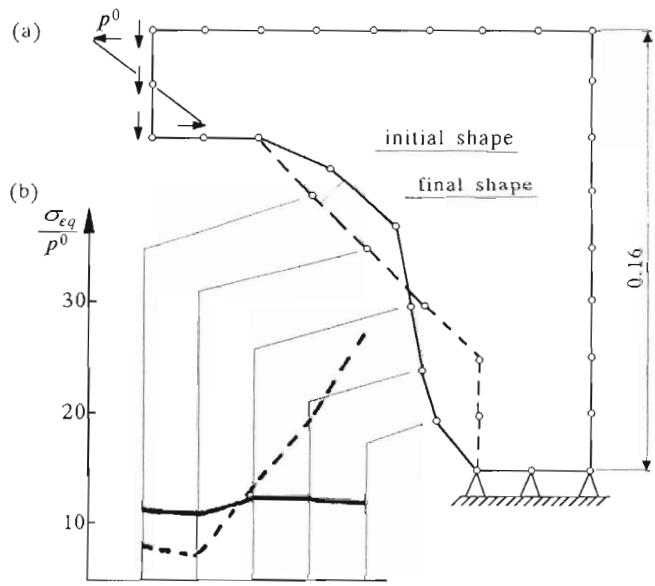

Fig. 5. Shape optimization of a steel corner

Example 5. *Shape optimization of a steel foot for the displacement constraint (see Burczyński, 1993a)*

The problem of shape optimization for the displacement constraint represented by

$$|u(x)| - u_0 \leq 0 \tag{5.2}$$

was considered. One assumed that displacements of the loaded boundary of a steel foot (Fig.6) should have not exceed the admissible value $u_0 = 0.055\,\mathrm{mm}$. The problem was replaced by minimization of the functional J_0

$$J_0 = \int_{\Gamma_2} \Big[\frac{|u(x)|}{u_0}\Big]^k d\Gamma_2 \qquad k = 100 \tag{5.3}$$

with the constraint in the form of constant area of the body. The boundary element model had 37 linear elements. The final optimal shape of the boundary was obtained in 8th iteration and the minimum of the functional ensured that displacements of all loaded boundary nodes were smaller than or equal to u_0.

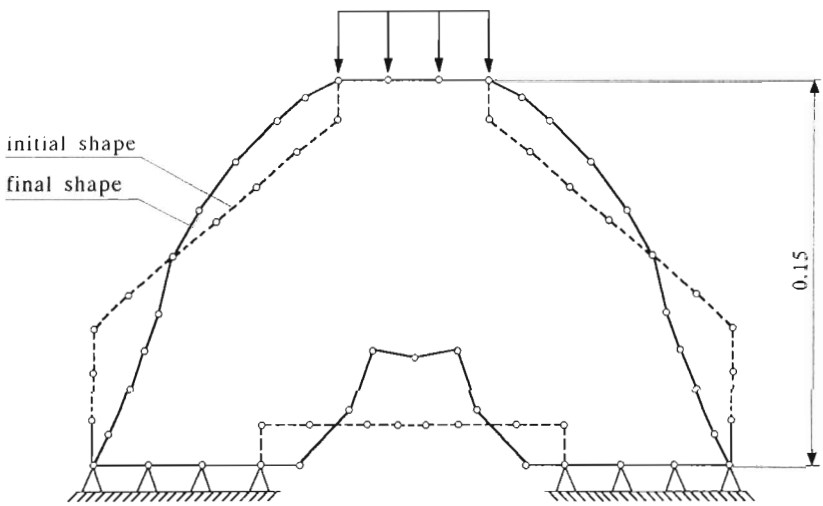

Fig. 6 Shape optimization of a steel foot

Example 6. *Shape optimization of a steel rectangular plate for the frequency criterion (see Burczyński and Fedeliński, 1990b)*

The problem of shape optimal design of the lower boundary of the steel plate mentioned in the example 3 was considered. The objective function was to maximize the first natural frequency subject to the cost constraint and some geometrical constraints. Three initial shapes, shown in Fig.7 were assumed. As the result of optimization the first natural frequency increased from 3116 to 3620 rad/s. Practically identical final shapes were obtained. It is seen that the material tends to *expand* near the support.

Acknowledgement

This paper presents the work which was carried out within the grant No. 8T11F00810 of the State Committee for Scientific Research (KBN).

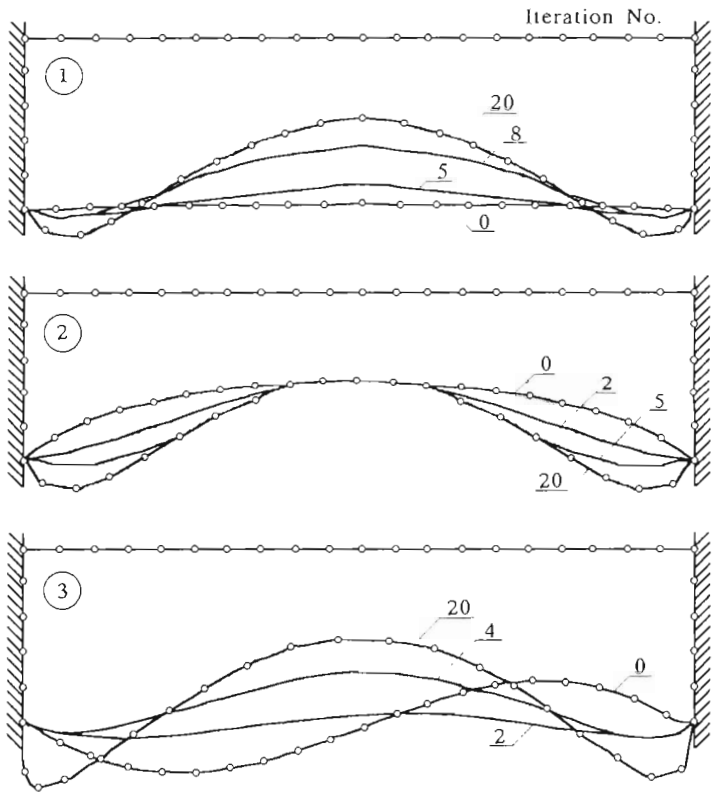

Fig. 7. Shape optimal design of a steel rectangular plate

References

1. BURCZYŃSKI T., 1993a, Applications of BEM in Sensitivity Analysis and Optimization, *Computational Mechanics*, **13**, 1/2, 29-44

2. BURCZYŃSKI T., 1993b, Recent Advances in Boundary Element Approach to Design Sensitivity Analysis – Survey, In: *Design Sensitivity Analysis* (edit. M.Kleiber, T.Hisada), Atlanta Technology Publications, Atlanta, 1-25

3. BURCZYŃSKI T., 1995, *The Boundary Element Method in Mechanics*, CAD/CAM Series, WNT Warsaw

4. BURCZYŃSKI T., BELUCH W., KUHN G., 1997a, Sensitivity Analysis of Cracked Structures Using Boundary Elements, *Proc. XIII Conference on Computer Methods in Mechanics*, Poznań, 213-220

5. BURCZYŃSKI T., FEDELIŃSKI P., 1990a, Shape Sensitivity Analysis of Natural Frequencies Using Boundary Elements, *Structural Optimization*, **2**, 1, 47-54

6. BURCZYŃSKI T., FEDELIŃSKI P., 1990b, Shape Sensitivity Analysis and Optimal Design of Static and Vibrating Systems Using the Boundary Element Method, *Control and Cybernetics*, **19**, 3/4, 47-71

7. BURCZYŃSKI T., FEDELIŃSKI P., 1992, Boundary Elements in Shape Design Sensitivity Analysis and Optimal Design of Vibrating Structures, *Engineering Analysis with Boundary Elements*, **9**, 195-202

8. BURCZYŃSKI T., HABARTA M., KOKOT G., 1996a, Coupling of the Boundary Elements and Path-Independent Integrals in Generalizaed Shape Optimization and Defect Identification, *Proc. 2nd International Conference on Inverse Problems in Engineering: Theory and Practice*, Le Croisic, France

9. BURCZYŃSKI T., HABARTA M, POLCH E.Z., 1996b, Boundary Element Formulation for Sensitivity Analysis and Detection of Cracks and Voids, In *Structural and Multidisciplinary Optimization* (edit. N.Olhoff, G.Rozvany), Pergamon Elsevier Science

10. BURCZYŃSKI T., KANE J.H., BALAKRISHNA C., 1995, Shape Design Sensitivity Analysis via Material Derivative-Adjoint Variable Techniques for 3-D and 2-D Curved Boundary Elements, *International Journal for Numerical Methods in Engineering*, **38**, 17, 2839-2866

11. BURCZYŃSKI T., KANE J.H., BALAKRISHNA C., 1997b, Comparison of Shape Design Sensitivity Analysis via Material Derivative-Adjoint Variable and Implicit Differentiation Techniques for 3-D and 2-D Curved Boundary Elements, *Computer Methods in Applied Mechanics and Engineering*, **142**, 89-109

12. BURCZYŃSKI T., KOKOT G., 1997, Topology Optimization Using Boundary Elements, *Proc. XIII Conference on Computer Methods in Mechanics*, Poznań, 221-228

13. BURCZYŃSKI T., KUHN G., ANTES H., NOWAKOWSKI M., 1997c, Boundary Element Formulation of Shape Sensitivity Analysis for Defect Identification in Free Vibration Problem, *Engineering Analysis with Boundary Elements*, **19**, 2, 167-175

14. BURCZYŃSKI T., NOWAKOWSKI M., 1997, Identification of Voids in Vibrating Structures, *Proc. XIII Conference on Computer Methods in Mechanics*, Poznań, 229-236

15. BURCZYŃSKI T., POLCH E.Z., 1994, Path-Independent and Boundary Integral Approach to Sensitivity Analysis and Identification of Cracks, In: *Inverse Problems in Engineering Mechanics* (edit. H.D.Bui, M.Tanaka et. al.), A.A. Balkema Publishers, Rotterdam, 355-361

16. DEMS K., MRÓZ Z., 1986, On a Class of Conservation Rules Associated with Sensitivity Analysis in Linear Elasticity, *Int. J. Solids and Structures*, **22**, 737-758

17. FEDELIŃSKI P., 1991, Application of the Boundary Element Method in Shape Optimization of Vibrating Mechanical Systems, Ph.D. Thesis, Mechanical Engineering Faculty, Silesian Technical University, Gliwice

18. MRÓZ Z., 1986, Variational Approach to Shape Sensitivity Analysis and Optimal Design, In: *The Optimum Shape-Automated Structural Design* (edit. J.A.Bennet, M.E.Botkin), Plenum Press, New York, 79-105

19. PORTELA A., 1993, *Dual Boundary Element Analysis of Crack Growth*, CMP, Southampton

Metoda elementów brzegowych w analizie wrażliwości, optymilizacji i identyfikacji

Streszczenie

W pracy przedstawiono zastosowanie metody elementów brzegowych w zagadnieniach analizy wrażliwości, optymilizacji i identyfikacji. Głównym celem artykułu jest przedstawienie w sposób ujednolicony powyższych zagadnień ze szczególnym uwzględnieniem uzyskanych w ostatnim okresie wyników obliczeń numerycznych.

Manuscript received December 19, 1997; accepted for print February 3, 1998